Tissue and Cell 103 (2026) 103713

Contents lists available at ScienceDirect

Tissue and Cell

journal homepage: www.elsevier.com/locate/tice

Trophoblast cell-surface antigen 2 evaluation in intraepithelial neoplasia and intraductal carcinoma of the prostate: An immunopathological study

Sonia Fantone [a,1,2], Giovanni Tossetta [b,1,3], Francesca Sanguedolce [c,4], Gaia Goteri [d,5], Daniela Marzioni [e,f,*,6,7], Roberta Mazzucchelli [d,6,8]

[a] Scientific Direction, IRCCS INRCA, Ancona 60124, Italy
[b] Department for the Promotion of Human Science and Quality of Life, San Raffaele University, Rome 00166, Italy
[c] Pathology Unit, Policlinico Foggia, University of Foggia, Foggia 71122, Italy
[d] Department of Biomedical Sciences and Public Health, United Hospitals, Università Politecnica delle Marche, Ancona 60126, Italy
[e] Department of Experimental and Clinical Medicine, Università Politecnica delle Marche, Ancona 60126, Italy
[f] IRCCS INRCA, Ancona 60124, Italy

ARTICLE INFO

Keywords:
Prostate cancer
Intraductal carcinoma of the prostate
Prostatic intraepithelial neoplasia
Trop-2

ABSTRACT

The origin of intraductal carcinoma of the prostate (IDC-P) in presence of prostate adenocarcinoma (PCa) is a matter of debate. This study evaluates trophoblast cell-surface antigen 2 (Trop-2) expression in prostatic high-grade intraepithelial neoplasia (HGPIN), IDC-P and PCa to explain the possible mechanism for IDC-P arising. Trop-2 was localized in the luminal epithelium of normal prostate gland, HGPIN and IDC-P. The quantitative analysis of immunohistochemistry showed no difference of Trop-2 expression between HGPIN and IDC-P, while statistically significant differences were observed comparing the two pathologies with normal tissues. Contrarily, Trop-2 was expressed in 2.5% of the basal cells in normal prostate gland and in 1% of HGPIN while Trop-2 was expressed in 8% of cells in IDC-P samples. We suggest that Trop-2 present in the basal cells may acquire neoplastic changes. The neoplastic cells could grow into the glandular lumen as HGPIN and/or spread into the duct as IDC-P or spread into the stroma as PCa. In conclusion, our data in part support the theory of intraductal carcinoma origin through retrograde glandular colonization.

1. Introduction

Prostate cancer (PCa) is the second most common cancer in men and the fifth most harmful. There are several risk factors that promote PCa development such as race, family history, germline mutations and age. More than half of PCa diagnosis occur in men of more than 65 years and increase significantly in the elderly so, aging can represent a risk factor (Bergengren et al., 2023; Ramakrishnan et al., 2023). The clinical spectrum of PCa encompasses indolent diseases with low risk of progression to highly aggressive disease that have recurrence and high rates of cancer-related death. It is known that invasive high-grade cancer is frequently associated with prostatic intraductal carcinoma (IDC-P), which is considered a distinct entity by WHO tumor classification of urinary system since 2016 (Amin MB et al., 2022). Morphologically, IDC-P is defined by the presence of a lumen-spanning proliferation of malignant secretory cells within pre-existing benign prostatic ducts and acini, with retention of basal cells (Montironi et al., 2018).

It is common knowledge that IDC-P presence in a prostate tissue

* Corresponding author at: Department of Experimental and Clinical Medicine, Università Politecnica delle Marche, Ancona 60126, Italy.
E-mail addresses: s.fantone@inrca.it (S. Fantone), giovanni.tossetta@uniroma5.it (G. Tossetta), francesca.sanguedolce@unifg.it (F. Sanguedolce), g.goteri@univpm.it (G. Goteri), d.marzioni@univpm.it (D. Marzioni), r.mazzucchelli@univpm.it (R. Mazzucchelli).
[1] Equally contributed as first author
[2] 0000-0002-5630-5984
[3] 0000-0001-7003-1230
[4] 0000-0001-7459-3521
[5] 0000-0001-5198-8387
[6] Equally contributed as last author
[7] 0000-0002-2267-0270
[8] 0000-0002-3058-4110

https://doi.org/10.1016/j.tice.2026.103713
Received 11 September 2025; Received in revised form 8 June 2026; Accepted 19 June 2026
Available online 20 June 2026
0040-8166/© 2026 The Author(s). Published by Elsevier Ltd. This is an open access article under the CC BY license (http://creativecommons.org/licenses/by/4.0/).

sample is linked to a poorer prognosis. The most IDC-P lesions were found near to invasive carcinoma with Gleason pattern 4 or 5 and linked to a large tumor volume and advanced stage, while IDC-P without PCa is a rare phenomenon (Porter et al., 2017; Robinson and Epstein, 2010; Watts et al., 2013). Currently, high grade prostatic intraepithelial neoplasm (HGPIN) is considered the only precursor of PCa. Both IDC-P and HGPIN retain basal cell layer and consist of malignant cells within the ducts and acini (Miyai et al., 2014; Zong et al., 2021).

Trophoblast Cell-Surface Antigen 2 (Trop−2) is a transmembrane glycoprotein belonging to the EpCAM (epithelial cell adhesion molecule) family of proteins (Koltai and Fliegel, 2023; Shen et al., 2021) and comprises an extracellular domain, a single hydrophobic transmembrane helix and a cytoplasmic C-terminal tail (Trerotola et al., 2013). Trop−2 is involved in various cellular functions such as proliferation, invasion, stemness and regulation of cell-cell adhesion (through its extracellular region) (Koltai and Fliegel, 2023).

The aim of this study was to evaluate Trop−2 expression in HGPIN, IDC-P and PCa to suggest a possible mechanism for IDC-P arising.

2. Materials and methods

2.1. Tissue collection

The study included a total of 20 paraffin embedded prostate tissues (10 IDC-P and 10 HGPIN, all associated with PCa) from radical prostatectomy provided by Pathological Anatomy service (Università Politecnica delle Marche–United Hospitals, Ancona, Italy). Prior to surgery the patients had not received antiandrogen therapy. All diagnosis were confirmed and selected by a pathologist (RM). Patients with IDC-P had an average age of 69 years (range 59–77) while the average age of patients with HGPIN was 66 years (range 56–75). All procedures followed were in accordance with the ethical standards of the committee responsible on human experimentation (institutional and national) and with the Helsinki Declaration of 1975, as revised in 2013. The study was approved by Territorial Ethics Committee (T.E.C.) of the Marche Region (IT) (approval reference number: 2024–135). The requirement for informed consent was waived because of the retrospective study design.

All clinical and pathological characteristics of patients were reported on Table 1.

Table 1
Clinical and pathological findings.

IDC-P cases	Age	PSA (ng/ml)	Gleason score (GG)*	pTNM**
1	73	4,4	5 + 4 = 9 (5)	T3b R1 LVI0 N1
2	66	2,4	3 + 4 = 7 (2)	T3a R0 LVI0 NX
3	77	22	4 + 3 = 7 (3)	T3a (m,2) R1 LVI0 N1
4	65	6,8	4 + 3 = 7 (3)	T3a (m,4) R0 LVI0 NX
5	59	7,9	4 + 3 = 7 (3)	T3b R0 LVI0 N0
6	72	6,8	4 + 3 = 7 (3)	T3b R0 LVI0 N1
7	79	8,9	4 + 4 = 8 (4)	T3a (m,2) R0 LVI0N0
8	61	4,8	3 + 4 = 7 (2)	T2 (m,2) R1 LVI0 NX
9	75	15	4 + 3 = 7 (3)	T3b (m,3) LVI0 N0
10	66	16,4	4 + 3 = 7 (3)	T3b R0 LVI0 N0
HGPIN cases				
1	74	3,3	3 + 3 = 6 (1)	T3a (m,3) R0 LVI0 NX
2	75	12	3 + 4 = 7 (2)	T3a (m,2) R1 LVI0 N0
3	72	4,25	3 + 3 = 6 (1)	T2 (m,2) R0 LVI0 N0
4	62	4,93	3 + 3 = 6 (1)	T2 (m,3) R0 LVI0 NX
5	67	6,11	3 + 4 = 7 (2)	T2 R1 LVI0 NX
6	66	5,2	3 + 3 = 6 (1)	T2 (m,3) R0 LVI0 NX
7	63	6,7	3 + 3 = 6 (1)	T2 (m,4) R0 LVI0 NX
8	64	6	3 + 4 = 7 (2)	T2 (m,2) R1 LVI0 NX
9	56	8,3	3 + 4 = 7 (2)	T2 (m,3) R0 LVI0 NX
10	62	7,7	3 + 4 = 7 (2)	T2 (m,3) R1 LVI0 NX

* GG: Grade Group; pTNM**: Pathological Tumor Node Metastasis based on AJCC 8°edition.

2.2. Peroxidase immunohistochemistry

The immunohistochemistry procedure for Trop−2 was performed as previously described (Licini et al., 2021). Negative controls were obtained by omitting the primary or secondary antibody or using an isotype control antibody (ab281590; Abcam, Cambridge, UK) at the same dilution of primary antibody for all the immunohistochemical reactions performed. P63/CK34βE12 (the basal cell cocktail (34bE12 +p63; Codes M731701–2, M063001–2, Dako Agilent Technologies) staining was performed to detect prostate basal cells as routinely used for diagnosis of PCa by the Pathological Anatomy Service.

2.3. Double staining and confocal microscopy

The double staining was performed as previously described (Licini et al., 2021). Sections were incubated overnight at 4°C with the primary antibodies anti-Trop−2 mouse monoclonal antibody (sc−376746, Santa Cruz Biotechnology, Inc., TX, USA) and anti-Cytokeratin 5 (CK5) rabbit polyclonal antibody (PA5–84421, Thermo Fisher Scientific) diluted 1:400 and 1:500, respectively, in PBS. Sections were then washed and incubated for 30 min at RT with the secondary antibodies anti-mouse (Trop−2) Alexa Fluor−488 and anti-rabbit (CK5) Alexa Fluor−555 (both from Invitrogen, Carlsbad, CA, USA) diluted 1:400. Slides were then incubated with DAPI (1:5000, Invitrogen) for 10 min for nuclear staining. Finally, sections were washed and mounted using Vectashield mounting medium (Vector Laboratories). Sections were analyzed with the inverted microscope Eclipse Ti2-E supplied with an AX confocal system (Nikon, Japan). The following detection setting was used: Detector PMT (405) and GaAsP (488 and 561) with 2x line averaging and bit depth= 12. Moreover, we used the following objectives:

- 10x/0.45 NA objective (Calibration: 0.86 μm/px)
- 20x/0.75 NA objective (Calibration: 0.43 μm/px)

The percentage of Trop−2-positive prostatic basal cells also expressing CK5 were calculated in 10 samples of each group (HGPIN and IDC-P). For the morphometry, four non-overlapping images from each section were randomly selected and analyzed.

2.4. Semi-quantitative and statistical analysis of samples

Semi-quantitative analysis of Trop−2 immunohistochemical staining and the quantitative analysis of the double positive (CK5-Trop−2) basal cells detected by immunofluorescence were performed in a blinded manner by taking four representative non-overlapped images from each of the 10 cases per group. For Trop−2 immunohistochemistry analysis was used the Nikon Eclipse E800 light microscope equipped with a Nikon DXM 1200 camera (Nikon Instruments S.p.A, Calenzano, Italy). Image-J (ver 1.54 s) software as reported in literature (Dai et al., 2020; Tossetta et al., 2025; Yang et al., 2021).

Results were represented as mean ± standard deviation (SD) of positive area (%), where % of positive area was calculated as follows:

$$\%of\ positive\ area = \frac{positive\ pixels\ of\ the\ field(area)}{total\ pixels\ of\ the\ field(area)} \quad x \quad 100$$

Field size was 650 × 480 μm for all images analyzed.

For immunofluorescence analysis was used the 20x/0.75 NA objective. The following number of cells was counted for each group: 1592 basal cells for normal prostate, 1388 basal cells for HGPIN and 620 basal cells for IDC-P.

Sample normality was assessed using the Shapiro-Wilk test before applying the Student's *t*-test and p values < 0.05 were considered statistically significant. All analyses were carried out using GraphPad Prism (ver 8) statistical software.

3. Results

3.1. Characterization of tissue samples from patients with prostate cancer

Normal prostate tissue was taken from the peripheral zone of the prostate at least 2 mm from the lesions (HGPIN and IDC-P) detectable in the same section. HGPIN was present both near and distant to PCa, in the same section. The identification of this preneoplastic lesion follows the morphological and immunohistochemical criteria of the WHO classification (Amin MB et al., 2022). We considered the three main form tufting, micropapillary and flat. We did not consider the cribriform pattern because it is now controversial (Epstein et al., 2021).

All cases of IDC-P were identified adjacent to PCa. Confirmation of IDC-P was achieved by using the morphological criteria of the 2016 edition of the WHO Classification of Tumors of the Prostate Gland (Amin MB et al., 2022) and the presence of the basal cells was confirmed as well as for normal glandular tissue and HGPIN by p63 and 34betaE12 cocktail (Fig. 1**a,c,e**).

3.2. Immunohistochemical expression of Trop−2 in normal prostate, HGPIN and IDC-P

Trop−2 was expressed in the normal glandular epithelium (Fig. 1**b**) as well as in the HGPIN (Fig. 1**d**) and IDC-P (Fig. 1**f**). In the normal glandular epithelium (Fig. 1**b**) and in HGPIN (Fig. 1**d**) the staining for Trop−2 is present on the cytoplasmatic membrane of the secretory cells in a basal-lateral fashion. Particularly, Trop−2 immunohistochemical expression was significantly higher in HGPIN ($p < 0.0001$) and IDC-P ($p < 0.0001$) than normal tissue while Trop−2 expression showed no difference between HGPIN and IDC-P (Fig. 1**g**). In addition, the staining of this marker in both normal glandular epithelium and in HGPIN appears homogeneous (Fig. 1**b,d**).

Unlike the previous ones, IDC-P showed a heterogeneous non-uniform staining for Trop−2 showing in some cases a less strong staining at the centre of lumen-spanning proliferation of malignant secretory cells than at the peripheral part (Fig. 1**f**). In addition, Trop−2 expression in IDC-P is like the expression of Trop−2 in adjacent PCa observed in the same sample (data not shown).

3.3. Immunofluorescence and confocal microscopy analysis

To better demonstrate the localization of Trop−2 in the epithelial layer of prostate gland we performed a double immunofluorescent staining using Trop−2 (green colour in Fig. 2) and CK5 (red colour in Fig. 2). The Fig. 2a, a' represent normal glands showing that Trop−2 (green staining) and CK5 (red staining) were colocalized in the 2.5% of basal cells. The colocalization (Trop−2 – CK5) was present in isolated randomly arranged cells (see Fig. 2 **a,a'**, the yellow staining demonstrates the colocalization, see the arrow). In addition, HGPIN (Fig. 2 **b, b'**) showed 1% of colocalization of Trop−2 and CK5 in our samples while IDC-P (Fig. 2 **c,c'**) showed 8% of cells expressing both Trop−2 and

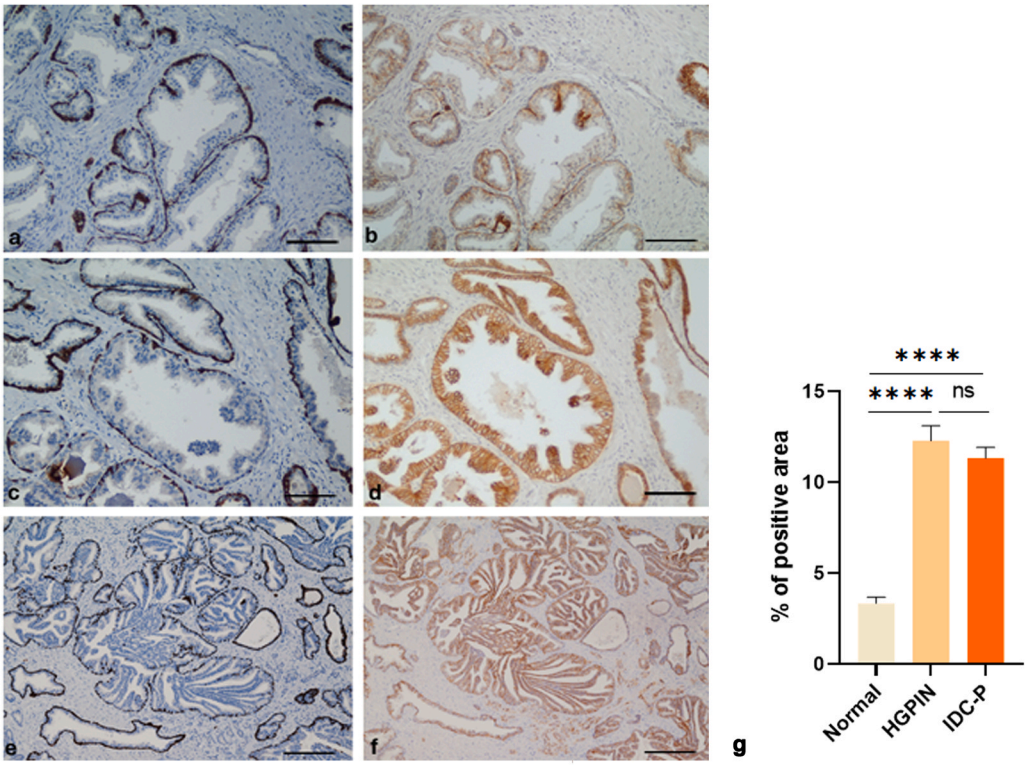


Fig. 1. Representative imagines of HGPIN and IDC-P samples. a, b show normal prostate gland; c, d show HGPIN and e, f show IDC-P. P63/CK34βE12 immunohistochemical staining (a, c, e); Trop−2 staining (b, d, f). P63/CK34βE12, used as a basal prostate cells marker, is present in the basal cells of normal prostate glands, HGPIN and IDC-P samples (a, c, e). Trop−2 staining is detectable in the epithelial cells of all the samples analyzed (b, d, f) while the stomal component is negative. Fig. 1g shows Trop−2 immunostaining quantification. Results were reported as bars of a histogram and represented as mean ± standard deviation (SD) of positive area (%). **** $p < 0.0001$, ns= Not statistically significant. a-d: bar= 100 μm; e and f, bar= 200 μm.

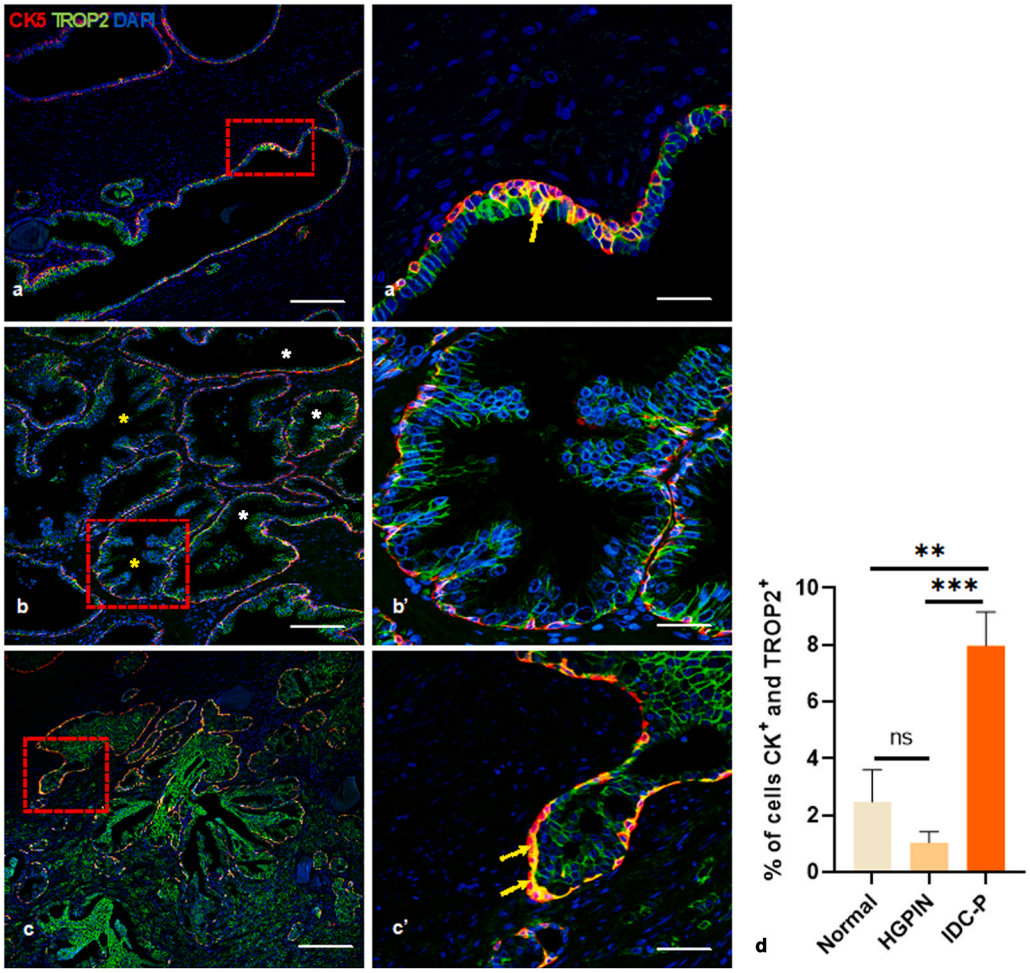


Fig. 2. Representative imagines of double staining of Trop−2 and CK5 in HGPIN and IDC-P samples by confocal microscopy. Normal prostate glands (a, a'); HGPIN (b, b') and IDC-P (c, c'). a', b' and c' are the enlargement of the framed area in a, b and c respectively; d) shows the percentage of cells stained for both CK and TROP2. The nuclei are stained in blue. CK5 (red staining) was used as a marker for prostate basal cells and Trop−2 (green staining) is localized in the secretory cells of normal glands, HGPIN and IDC-P. In figure b, most of the HGPIN (see yellow asterisks) are on the left while the normal component (see white asterisks) is observable on the right in the image. The figure b' shows an enlargement of HGPIN. Trop−2 is localized in sporadic basal cells of normal glands (yellow staining and arrow: a') and in some cells in IDC-P (yellow staining and arrows: c'). Results were reported as bars of a histogram and represented as mean percentage of double stained cells ± standard deviation (SD). ** $p < 0.01$, *** $p < 0.001$, ns= Not statistically significant. a-c bar= 200 μm; a', b' bar= 45 μm; c' bar= 40 μm.

CK5.

So, we can conclude that Trop−2, in basal cells, is statistically significant more expressed in IDC-P compared to normal glands ($p < 0.01$) and HGPIN samples ($p < 0.001$; Fig. 2d). No statistically significant differences were found between normal glands and HGPIN (Fig. 2d). Trop−2 was homogenously expressed in the luminal epithelium of the gland in normal, HGPIN and IDC-P samples. No expression of CK5 was visible in PCa.

4. Discussion

In the present study, we investigated the expression of Trop−2 in HGPIN and IDC-P. The semi-quantitative analysis of Trop−2 immunohistochemistry showed no significant differences between HGPIN and IDC-P while significant differences were shown comparing these pathologies with normal tissues. It is known that morphological and molecular abnormalities detected in PCa are like that shown in secretory cells of both HGPIN and IDC-P (Bernhardt, M., Kristiansen, G. 2023). For example, HGPIN and IDC-P share cytological features such as nuclear enlargement, prominent nucleoli, and cellular crowding like PCa. In addition, HGPIN and IDC-P frequently share molecular signatures found in PCa, including TMPRSS2-ERG gene fusions, AMACR overexpression, and specific genetic mutations (Amin MB et al., 2022).We have detected for the first time that Trop−2 was in luminal cells and only in 2.5% of basal cells of the normal epithelial glands and in 8% of basal cells of IDC-P using appropriate basal cell marker and confocal microscopy. The precise location of Trop−2 may be important to understand the relationship between IDC-P and the adjacent PCa. Recently, Wang et al. (Wang et al., 2024) performed a study on the feasibility of Antibody-Drug Conjugates of different targets including Trop−2, in Ductal Adenocarcinoma (DAC) and IDC-P. This study reports that Trop−2 expression in IDC-P and DAC is like the expression of Trop−2 in adjacent PCa as we have observed in our samples. The presence of multiple basal cells expressing Trop−2 (8%) in the IDC-P may suggest an anomalous condition linked to the onset of the pathology. Trop−2 expression in the basal cells may be related to the acquisition of neoplastic changes. The neoplastic cells could grow into the glandular lumen and/or spread into the duct as IDC-P or spread into the stroma as PCa. The presence of these Trop−2 stained cells in the basal layer could represent prostatic cancer stem cells (PCSC) cancer-initiating and it can partially support the theory of intraductal carcinoma origin through retrograde glandular colonization (Bernhardt and Kristiansen, 2023; Haffner et al., 2016) and to confirm that Trop−2 is involved in PCa origin (Guerra et al., 2021). PCa may originate from the same cell in

particular environmental conditions such as mutations, virus and other genetic and not genetic factors (Guerra et al., 2023; McDougall et al., 2015). The interpretation of these data can be considered a suggestion for future *in vitro* investigation as our research is based exclusively on morphological data. Thus, the latter and a limited analysed cohort can represent the limitations of the current study.

5. Conclusions

In conclusion, our data suggest that future in vitro studies could be conducted to prove our morphological observation concerning the hypothesis that the IDC-P and PCa might originate from the same cell type located in the basal layer of the prostate gland that expresses Trop−2, while a different mechanism could be responsible for the HGPIN occurrence. In addition, the modulation of the prostatic environment, such as non-mutagenic mechanisms or mutagenic oncogenic events or both can drive tumour progression inducing these cells to proliferate and differentiate in an anomalous way both by taking the intraductal and prostatic stroma routes, evolving into IDC-P and PCa respectively.

CRediT authorship contribution statement

Giovanni Tossetta: Writing – original draft, Visualization, Resources, Methodology. **Sonia Fantone:** Writing – original draft, Visualization, Resources, Methodology. **Gaia Goteri:** Writing – review & editing, Visualization. **Francesca Sanguedolce:** Writing – review & editing, Visualization. **Roberta Mazzucchelli:** Writing – review & editing, Visualization, Supervision, Conceptualization. **Daniela Marzioni:** Writing – review & editing, Visualization, Supervision, Conceptualization.

Funding

This work did not receive any external fundings.

Declaration of Competing Interest

The authors declare no competing interests

Acknowledgments

We thank Dr. Tatiana Spadoni and Prof. Laura Graciotti (Center of Confocal and Electronic Microscopy and CLEM, Department of Biomedical Sciences and Public Health, Polytechnic University of Marche, Ancona, Italy) for confocal images.

Data availability

No data was used for the research described in the article.

References

Amin MB, K.J.R.M., Srigley, J.R., Tsuzuki, T., 2022. Tumours of the prostate. Urinary and Male Genital Tumours. WHO Classification of Tumors, 5th ed. International Agency for Research on Cancer, Lyon, France, pp. 194–234.

Bergengren, O., Pekala, K.R., Matsoukas, K., Fainberg, J., Mungovan, S.F., Bratt, O., Bray, F., Brawley, O., Luckenbaugh, A.N., Mucci, L., Morgan, T.M., Carlsson, S.V., 2023. 2022 Update on prostate cancer epidemiology and risk factors-a systematic review. Eur. Urol. 84 (2), 191–206. https://doi.org/10.1016/j.eururo.2023.04.021.

Bernhardt, M., Kristiansen, G., 2023. Molecular alterations in intraductal carcinoma of the prostate. Cancers (Basel) 15 (23). https://doi.org/10.3390/cancers15235512.

Dai, Z., Song, G., Balakrishnan, A., Yang, T., Yuan, Q., Mobus, S., Weiss, A.C., Bentler, M., Zhu, J., Jiang, X., Shen, X., Bantel, H., Jaeckel, E., Kispert, A., Vogel, A., Saborowski, A., Buning, H., Manns, M., Cantz, T., Ott, M., Sharma, A.D., 2020. Growth differentiation factor 11 attenuates liver fibrosis via expansion of liver progenitor cells. Gut 69 (6), 1104–1115. https://doi.org/10.1136/gutjnl-2019-318812.

Epstein, J.I., Amin, M.B., Fine, S.W., Algaba, F., Aron, M., Baydar, D.E., Beltran, A.L., Brimo, F., Cheville, J.C., Colecchia, M., Comperat, E., da Cunha, I.W., Delprado, W., DeMarzo, A.M., Giannico, G.A., Gordetsky, J.B., Guo, C.C., Hansel, D.E., Hirsch, M. S., Huang, J., Humphrey, P.A., Jimenez, R.E., Khani, F., Kong, Q., Kryvenko, O.N., Kunju, L.P., Lal, P., Latour, M., Lotan, T., Maclean, F., Magi-Galluzzi, C., Mehra, R., Menon, S., Miyamoto, H., Montironi, R., Netto, G.J., Nguyen, J.K., Osunkoya, A.O., Parwani, A., Robinson, B.D., Rubin, M.A., Shah, R.B., So, J.S., Takahashi, H., Tavora, F., Tretiakova, M.S., True, L., Wobker, S.E., Yang, X.J., Zhou, M., Zynger, D. L., Trpkov, K., 2021. The 2019 Genitourinary Pathology Society (GUPS) White Paper on Contemporary Grading of Prostate Cancer. Arch. Pathol. Lab. Med. 145 (4), 461–493. https://doi.org/10.5858/arpa.2020-0015-RA.

Guerra, E., Di Pietro, R., Stati, G., Alberti, S., 2023. A non-mutated TROP2 fingerprint in cancer genetics. Front. Oncol. 13, 1151090. https://doi.org/10.3389/fonc.2023.1151090.

Guerra, E., Trerotola, M., Relli, V., Lattanzio, R., Tripaldi, R., Vacca, G., Ceci, M., Boujnah, K., Garbo, V., Moschella, A., Zappacosta, R., Simeone, P., de Lange, R., Weidle, U.H., Rotelli, M.T., Picciariello, A., Depalo, R., Querzoli, P., Pedriali, M., Bianchini, E., Angelucci, D., Pizzicannella, G., Di Loreto, C., Piantelli, M., Antolini, L., Sun, X.F., Altomare, D.F., Alberti, S., 2021. Trop-2 induces ADAM10-mediated cleavage of E-cadherin and drives EMT-less metastasis in colon cancer. Neoplasia 23 (9), 898–911. https://doi.org/10.1016/j.neo.2021.07.002.

Haffner, M.C., Weier, C., Xu, M.M., Vaghasia, A., Gurel, B., Gumuskaya, B., Esopi, D.M., Fedor, H., Tan, H.L., Kulac, I., Hicks, J., Isaacs, W.B., Lotan, T.L., Nelson, W.G., Yegnasubramanian, S., De Marzo, A.M., 2016. Molecular evidence that invasive adenocarcinoma can mimic prostatic intraepithelial neoplasia (PIN) and intraductal carcinoma through retrograde glandular colonization. J. Pathol. 238 (1), 31–41. https://doi.org/10.1002/path.4628.

Koltai, T., Fliegel, L., 2023. The Relationship between Trop-2, Chemotherapeutic Drugs, and Chemoresistance. Int. J. Mol. Sci. 25 (1). https://doi.org/10.3390/ijms25010087.

Licini, C., Avellini, C., Picchiassi, E., Mensa, E., Fantone, S., Ramini, D., Tersigni, C., Tossetta, G., Castellucci, C., Tarquini, F., Coata, G., Giardina, I., Ciavattini, A., Scambia, G., Di Renzo, G.C., Di Simone, N., Gesuita, R., Giannubilo, S.R., Olivieri, F., Marzioni, D., 2021. Pre-eclampsia predictive ability of maternal miR-125b: a clinical and experimental study. Transl. Res. 228, 13–27. https://doi.org/10.1016/j.trsl.2020.07.011.

McDougall, A.R., Tolcos, M., Hooper, S.B., Cole, T.J., Wallace, M.J., 2015. Trop2: from development to disease. Dev. Dyn. 244 (2), 99–109. https://doi.org/10.1002/dvdy.24242.

Miyai, K., Divatia, M.K., Shen, S.S., Miles, B.J., Ayala, A.G., Ro, J.Y., 2014. Clinicopathological analysis of intraductal proliferative lesions of prostate: intraductal carcinoma of prostate, high-grade prostatic intraepithelial neoplasia, and atypical cribriform lesion. Hum. Pathol. 45 (8), 1572–1581. https://doi.org/10.1016/j.humpath.2014.03.011.

Montironi, R., Zhou, M., Magi-Galluzzi, C., Epstein, J.I., 2018. Features and Prognostic Significance of Intraductal Carcinoma of the Prostate. Eur. Urol. Oncol. 1 (1), 21–28. https://doi.org/10.1016/j.euo.2018.03.013.

Porter, L.H., Lawrence, M.G., Ilic, D., Clouston, D., Bolton, D.M., Frydenberg, M., Murphy, D.G., Pezaro, C., Risbridger, G.P., Taylor, R.A., 2017. Systematic Review Links the Prevalence of Intraductal Carcinoma of the Prostate to Prostate Cancer Risk Categories. Eur. Urol. 72 (4), 492–495. https://doi.org/10.1016/j.eururo.2017.03.013.

Ramakrishnan, A., Datta, I., Panja, S., Patel, H., Liu, Y., Craige, M.W., Chu, C., Jean-Marie, G., Oladoja, A.R., Kim, I., Mitrofanova, A., 2023. Tissue-specific biological aging predicts progression in prostate cancer and acute myeloid leukemia. Front. Oncol. 13, 1222168. https://doi.org/10.3389/fonc.2023.1222168.

Robinson, B.D., Epstein, J.I., 2010. Intraductal carcinoma of the prostate without invasive carcinoma on needle biopsy: emphasis on radical prostatectomy findings. J. Urol. 184 (4), 1328–1333. https://doi.org/10.1016/j.juro.2010.06.017.

Shen, M., Liu, S., Stoyanova, T., 2021. The role of Trop2 in prostate cancer: an oncogene, biomarker, and therapeutic target. Am. J. Clin. Exp. Urol. 9 (1), 73–87.

Tossetta, G., Fantone, S., Filosa, A., Tomasini, C.F., Savoia, P., Marzioni, D., 2025. Psoriasis and lichen planus: an immunohistochemical study of Trophoblast cell-surface antigen 2 expression in skin biopsies. Hum. Cell. 38 (6), 179. https://doi.org/10.1007/s13577-025-01313-9.

Trerotola, M., Jernigan, D.L., Liu, Q., Siddiqui, J., Fatatis, A., Languino, L.R., 2013. Trop-2 promotes prostate cancer metastasis by modulating beta(1) integrin functions. Cancer Res. 73 (10), 3155–3167. https://doi.org/10.1158/0008-5472.CAN-12-3266.

Wang, X., Qi, L., Chen, M., Zhang, Y., Gao, X., Cai, Y., 2024. Feasibility study of ADCs targeting TROP-2, HER2, and CD46 in Ductal Adenocarcinoma and Intraductal Carcinoma of the prostate. World J. Urol. 42 (1), 404. https://doi.org/10.1007/s00345-024-05109-8.

Watts, K., Li, J., Magi-Galluzzi, C., Zhou, M., 2013. Incidence and clinicopathological characteristics of intraductal carcinoma detected in prostate biopsies: a prospective cohort study. Histopathology 63 (4), 574–579. https://doi.org/10.1111/his.12198.

Yang, T., Poenisch, M., Khanal, R., Hu, Q., Dai, Z., Li, R., Song, G., Yuan, Q., Yao, Q., Shen, X., Taubert, R., Engel, B., Jaeckel, E., Vogel, A., Falk, C.S., Schambach, A., Gerovska, D., Arauzo-Bravo, M.J., Vondran, F.W.R., Cantz, T., Horscroft, N., Balakrishnan, A., Chevessier, F., Ott, M., Sharma, A.D., 2021. Therapeutic HNF4A mRNA attenuates liver fibrosis in a preclinical model. J. Hepatol. 75 (6), 1420–1433. https://doi.org/10.1016/j.jhep.2021.08.011.

Zong, Y., Montironi, R., Massari, F., Jiang, Z., Lopez-Beltran, A., Wheeler, T.M., Scarpelli, M., Santoni, M., Cimadamore, A., Cheng, L., 2021. Intraductal carcinoma of the prostate: pathogenesis and molecular perspectives. Eur. Urol. Focus. 7 (5), 955–963. https://doi.org/10.1016/j.euf.2020.10.007.